Regular Article

Bacterial suspensions under flow

Eric Clement[1,a], Anke Lindner[1], Carine Douarche[2], and Harold Auradou[3]

[1] PMMH, UMR7636 CNRS – ESPCI – University Pierre et Marie Curie – University
Denis Diderot, 10 rue Vauquelin, 75005 Paris, France
[2] Laboratoire de Physique des Solides, Université Paris-Sud, CNRS UMR 8502,
91405 Orsay, France
[3] Univ Paris-Sud, CNRS, Lab FAST, Bât 502, Campus Univ Orsay, 91405 Orsay, France

Abstract. Fluids laden with motile bacteria enter in the category of
active matter, a new field currently developing at the convergence of
biology, hydrodynamics and statistical physics. Such suspensions were
shown recently to exhibit singular macroscopic transport properties. In
this paper we review some recent results, either theoretical or experi-
mental, on the active fluid rheology. We focus principally on bacteria
suspensions and the objective is to provide the basis for understanding
the emergence of the singular constitutive relations characterizing the
macroscopic transport properties of such an active fluid under flow.

1 Introduction

Animals locomotion displays fascinating collective properties originating from inter-
play between individual self-propulsion and interactions among individuals in the
group [1]. The notion of interaction is in itself a complex issue. It involves local order-
ing through contacts or longer range interactions mediated by the surrounding fluid
and also, something more behavioural implying chemical sensing or cognitive deci-
sion. In spite of the large lexical variety describing these phenomena (mobs, herds,
flocks, shoals, swarms), that applies to different animals moving in concert at different
scales, it is only recently that physicists have elaborated the paradigmatic concept
of active fluids. This notion enforces the statistical physics credo that *more is dif-
ferent* [2] meaning that at some scales will emerge a unified physical entity ruled by
macroscopic transport equations associated with constitutive relations. However, the
nature of the emergent fields (stress, velocity, density), usually coupled with order
parameters describing the local interaction processes, differs strongly from what is
currently known for the standard physics of fluids. Theoretically, the phenomeno-
logical approaches highlight that due to the intrinsic symmetries of the microscopic
interactions and the activity stemming from self-propulsion, many well-accepted no-
tions describing matter at thermal equilibrium should be deeply revisited [3].

Fluids loaded with swimming micro-organisms are systems of choice to study
these problems [4]. In recent studies, bacterial fluids were shown to revisit classical

---

[a] e-mail: eric.clement@upmc.fr

equilibrium properties of matter such as Brownian motion [5–7], Ficks law [8,9,11], spontaneous collective organization and low-Reynolds turbulence [13–16], and viscous response [17–19,54]. Experimentally these systems are rather easy to control and the recent advances in microfluidic technologies open the possibilities to fabricate environments where the biological activity and the motion in a flow can be assessed and controlled with great reliability [10–12]. Therefore, a true bottom/up approach of those active suspensions can be undertaken in order to establish the micro/macro passage on firm experimental ground.

The aim of the present review is to offer a synthetic presentation on bacterial suspensions viewed as an active fluid and also to describe some our recent experimental results illustrating the emergence of constitutive relations for bacterial suspensions under flow. This presentation is made in the context of recent advances in statistical mechanics of active suspensions developed from microscopic kinetic models hence providing a fundamental basis to describe the very peculiar rheology of active fluids at a macroscopic scale.

2 The small force kingdom

2.1 Swimming strategies

Due to their sizen, micro-organisms or active colloids moving in a fluid, cannot rely on inertia to propel autonomously. The fastest ones, can swim up to 10 times their body size in a second. Consequently, the corresponding Reynolds number is quite small (10^{-5}–10^{-3}). The motility is thus governed by the Stokes equations (see the review by Winkler et al. [68] in this series).

$$- \boldsymbol{\nabla} P + \eta \nabla^2 \boldsymbol{u} = 0 \tag{1}$$

$$\boldsymbol{\nabla}.\boldsymbol{u} = 0 \tag{2}$$

where P and $\boldsymbol{u}$ are the fluid pressure and velocity. The Stokes equation for which time explicitly disappears, induces many important consequences for the propelling strategies. The most striking one is that any reciprocal motion implying the swimmer boundaries can not lead to net motion. This is called the "reciprocal theorems" or sometimes the "scallop theorem" [20]. To break the time reversibility there are few strategies developed through evolution by the micro-organisms (for a review see for ex. Lauga et al. [21] or the book by Childress [22] and refs inside). For example, a backward undulating wave via the beating of a flagellum produces a forwards motion such as for sperms (see the review by Kaupp et al. [69] in this series). Generally, the production of waves, either tangential or normal to a body surface can be used for swimming at zero Reynolds. Such a scheme is developed by paramecia that can trigger metachronal surface waves of a cilia carpet in either direction, to move forwards and backwards. Also, some micro-organisms such as the mono-cellular algae *Chlamydomonas Reinhardtii* (eukaryotic organism, well studied by biologists) use two frontal flagella to swim a "breast-stroke" (see the review by Polin et al. [70] in this series), meaning that the flagellum shape changes in different parts of the swimming cycle in order to induce a non-reciprocal motion. There is however another important case developed by many prokaryotes (essentially bacteria) lacking the possibility to activate internally a flagellum, contrarily to eukaryotic cells. Those micro-organisms use the rotation of helicoidal flagella attached to the body via a nano scale rotary motor [23]. The right association of the motor rotation and the flagellum helical handedness creates a thrust on the body coming from the back. It is important to see that, the case of *Chlamydomonas Reinhardtii* it is exactly the opposite, the body is pulled

forwards by the flagella apparatus. Therefore both situations correspond respectively to "pusher" and "puller" swimming strategies and we will develop in the following, important hydrodynamical consequences based on this fact.

2.2 Scale of the driving forces

If a micro-organism swims autonomously in a fluid, the necessary momentum conservation implies that there can not be any net force nor net torque acting on the fluid. Therefore, if there is a pushing (or pulling) force acting externally on the body there has to be an exactly opposite force acting on the propelling apparatus, essentially coming from the body drag resistance to motion. The same reasoning stands for torque. By law of action and reaction a thrust with a force f means of course a similar force counteracting on the surrounding fluid (with the opposite sign). At this point, it is important to notice that for any fluid, there is an intrinsic force scale F associated with the value of the viscosity η_0 and the mass density ρ: $F = \eta_0^2/\rho$. For an object of size l moving in the fluid at a velocity V_0, the ratio of momentum diffusion time to inertia time at this length scale, defines the dimensionless Reynolds number: $Re = \rho l V_0/\eta_0$. Therefore, motion at finite Reynolds number requires forces of typical magnitude:

$$f = Re\ F = Re\ \eta_0^2/\rho. \tag{3}$$

Since the motion takes place at low Reynolds numbers, these forces are generically small with respect to the intrinsic fluid force scale (i.e. the "small force kingdom"). From the biological point of view, it is a source of energetic expense, crucial to assure motility and survival of the micro-organism. However, quantitatively, one must realize that the propulsive power is not likely to affect much the global cell metabolism, only few percent of its energetic budget [20]. Put in the pleasant phrasing of E.M. Purcell – in the midst of the 1970's oil crisis – a motile bacterium would feel "like driving a Datsun in Saudi Arabia". Indeed this has practical importance for the "minimal media" usually used as the surrounding fluid in which the bacterial suspension is prepared. This preparation is essentially composed of amino-acids and low sugar sources for energy. In response to this diet, the bacteria would rather give-up splitting or making biofilms out of extracellular matrix production, two energetically expensive activities, but keep on swimming actively. This is how in practice controllable active suspensions are prepared. Let us consider for example, a bacterium like *Escherichia Coli* (*E.coli*) self-propelling at a velocity around $V_0 = 25\,\mu$m/s via a bundle of half a dozen of flagella. The body size is typically $a = 2\,\mu$m. Therefore in water, the Reynolds number is $Re \approx 10^{-4}$ and the propelling force is $f \approx 0.1\,pN$. The energy needed to move fluid elements on the order of a bacterium size $l \approx 10\,\mu$m (now including the flagella) is:

$$\sigma_0 = fl \propto \eta_0 V_0 l^2. \tag{4}$$

This important energy scale is often called the "dipolar strength", a name which justification will be exposed in the next sub-chapter. From the mechanical point of view the dipolar strength is a central characterization of the organism motile activity. *E.coli* for example, yields $\sigma_0 \approx 10^{-18}$ J, a value overcoming by 2–3 three orders of magnitudes the thermal energy scale ($k_B T$). For such bacteria, the propulsion velocity is directly associated with the motor rotation rate: $V_0 \propto \Omega$. The proportionality factor is a microscopic length scale depending only on the geometrical characteristics of the swimmer. It is important to see that the fluid viscosity scales-out of this picture provided that the motor rotation rate can be held constant by the bacterium activity. This is almost the case in standard conditions and thus, in a large range of viscosities, a bacterium is able to provide enough torque to maintain a fixed rotation rate and thus a constant swimming velocity (see Martinez et al. [24] and refs inside).
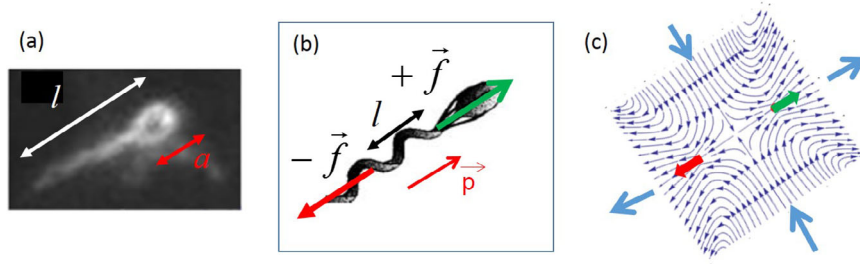
Fig. 1. Swimming *E.coli* bacterium (a) image of the swimming *E.coli* (ATCC9637) by fluorescent labelling of the body and the flagella. The body size is $a \approx 1.8\,\mu$m and the total length, including the flagella bundle $l \approx 10\,\mu$m. (b) Hydrodynamic representation of the bacterium as a "pusher" force dipole. (c) Resulting flow field created by the force dipole acting on the fluid. The blue arrows represent the main directions of the flow induced by the swimmer.

2.3 Autonomous swimmers as force dipoles

The fluid velocity field created by a moving bacterium is a-priori difficult to estimate in full details (see however, remarkable micro PIV measurements around micro-organisms *E.coli* [27] and Chlamidomonas [25,26]). As a generic feature for the Stokes equations solutions for an isolated swimming bacterium, the flow field can be expanded asymptotically at large distances, as a series of force multipoles. At the lowest order of expansion, the dominant term is a force dipole (a stresslet), inducing in the bacterium reference frame, a flow field:

$$\boldsymbol{u} = \epsilon \frac{\sigma_0}{8\pi\eta_0 r^3}(1 - 3cos\theta^2)\boldsymbol{r} \tag{5}$$

and a pressure:

$$P = \epsilon \frac{\sigma_0}{4\pi r^3}(1 - 3cos\theta^2) \tag{6}$$

where θ is the angle between the swimming direction and the radius vector $\boldsymbol{r}$, centred on the bacterium. The magnitude of the dipole is characterized by the dipolar strength σ_0. It is equivalent to two opposite forces of magnitude f acting on the fluid along the motion direction and separated by a distance l; the centre is at a mid-distance from the points of application of the forces. Expressions (5) and (6) correspond to the far-field limit. Note that here, we simply identify this scale l with the total swimmer size. This should not be taken to literally, as in reality the effective hydrodynamic size best characterizing the flow field from large scale to intermediate scale (as in Fig. 1(c)), should have a value between the body size and the total swimmer size. Hence, $\sigma_0 = fl$ and the two possible directions for the applied forces are given by the sign of ϵ. For "pusher type" swimmers $\epsilon = -1$ and for pullers $\epsilon = 1$. The structure of the fluid motion surrounding the swimming bacterium is a crucial element to keep in mind as it has important consequences on the emerging properties of the active fluid. For pusher swimmers, the induced fluid motion goes along the swimming direction in the front and is opposite in the tail. Also, the flow moves laterally towards the centre of the bacterium. Sometimes, such flow is called "extensile" (see Fig. 1). For pullers it is the reverse flow direction and the situation is called "contractile" [4]. Also, in some cases, the effective dipolar term may cancel and higher order multipolar contributions should come into play.

2.4 Run & tumble strategy for chemotaxis

As wild-type species (i.e. not genetically modified), most micro-organisms organize their motility as regular changes of swimming directions. The aim of this wandering motion is to explore and harvest the environmental resources and eventually find the right ecological niche. At low Reynold's number such a directional change has to be accompanied with a shape modification suited to produce a torque on the body. The alternation of directed motion and directional changes is called "run & tumble". For *E.coli* this strategy has been extensively studied. Following a biological signal, some motors changes their rotation direction yielding a partial or complete unbundling of the flagella; hence resulting in a reorientation of the swimming direction. According to the pioneering work of Berg [23], in chemically homogeneous conditions the run times and tumble times are distributed stochastically as Poisson variables with typical values $t_{run} \approx 1\,\mathrm{s}$ and $t_{tmb} \approx 0.1\,\mathrm{s}$ [23]. Interestingly, using tumbling mutants Saragosti et al. [28] have shown that the reorientation dynamics appears as a random walk on a unit sphere characterized by a rotational diffusion coefficient D_r. This authors argue that for a wild type, the resulting angular distribution for the redirection angles after tumbling $P(\theta)$ (as measured originally by Berg [30]), can be seen as the solution of a rotational diffusion equation corresponding to a rotational diffusion constant $D_r = 3.5\,\mathrm{rd}^2/\mathrm{s}$ and a mean tumbling time $t_{tmb} = 0.14$ ($D_r t_{tmb} \approx 0.5$). The mean tumbling direction is $<\theta> \approx 68°$. In those conditions, the compound of run & tumble motions induces on the long run, a diffusive motion characterized by a translational diffusivity:

$$D_t = \frac{1}{3}\frac{V_0^2 t_{run}}{1- <cos\theta>} \approx \frac{V_0^2 t_{run}}{6 D_r t_{tmb}}. \tag{7}$$

Thus following the trajectories of individual bacteria (or other micro-organisms) and averaging their mean-square displacements is a useful way to assess and characterize their activity. For non biased 3D isotropic motion, the mean-square displacement $<R^2>$ increases with the time-lag τ, as:

$$<R^2> = 6 D_t(\tau - \tau_c(1 - e^{-\tau/\tau_c})). \tag{8}$$

At long times, the diffusive motion: $<R^2> = 6 D_t \tau$, is recovered. However, at short times, a ballistic regime such that $<R^2> = V_0^2 \tau^2$, is observed and $D_t = \frac{1}{3}V_0^2 \tau_c$ where τ_c is the crossover time. In practice, using a 2 parameter fit equation (as Eq. (8)) the mean swimming velocity can be characterized as well as the long time diffusivity of the micro-organisms as a function of the environmental conditions (see examples of such measurements displayed in Fig. 4).

Note another useful complementary technique developed recently to characterize and monitor the mean activity of micro-organism suspensions. This technique called Differential Dynamic Microscopy (DDM), is based on the measurement of the spatio-temporal fluctuations of the average emitted light intensity and allows for high though-put measurements (see for ex. Martinez et al. and refs inside [29]).

For wild type *E.coli*, in nominal conditions, the translational diffusivity is $D_t \approx 100\,\mu\mathrm{m}^2/\mathrm{s}$. This is to be related to the typical Brownian motion, computed for a $2\,\mu m$ diameter sphere (at $300\,\mathrm{K}$): $D_B = 0.2\,\mu\mathrm{m}^2/\mathrm{s}$, a typical value for inactive *E.coli*. The rotational diffusivity ($D_r \approx 3\,\mathrm{rad}^2/\mathrm{s}$) can be compared to the typical values undertaken by an elongated passive rod of size $l \approx 5\text{–}10\,\mu m$: $D_r^{rod} \approx k_B T/\eta_0 l^3 \approx 10^{-2}\text{–}10^{-3}\,\mathrm{rad}^2/\mathrm{s}$. Therefore, in spite of the fact that it is not totally clear what should be the actual length contributing to the rotational Brownian motion, for wild type species, the disorientation process is essentially controlled by the tumbling activity. Note that for some micro-organisms, the tumbling motion can be triggered

by a mechanism different from a de-bundling process. For example, for marine bacteria *Vibrio alginolyticus* a flow triggered flagellar bucking is responsible for the change of direction [31] whereas for *Chlamydomonas Reinhardtii* a desynchronising process in the beating of the frontal flagella [32] triggers the reorientation (see the review by Polin et al. [70] in this series).

In a non uniform chemical environments, for example in a gradient of chemical attractants (or repellents), micro-organisms adapt the run and tumble times to the result of the environmental exploration [23]. *E.coli* possesses a fine biochemical sensing equipments which trigger internal biological cascades and control the rate of reversal for the rotation of the nano-motor driving the flagella [33]. Thus, by enhancing the run time and/or diminishing the tumble time, this micro-organism is able to produce a net motion in the direction of gradients of attractants (or against if it is a repellent). This ability to follow chemical gradients is called chemotaxis [36]. For an extensive account of models describing mathematically the chemotactic behaviour see for example [34] and [35] and refs inside. Note that for a run and tumble strategy to make any sense, the bacteria have to move straight during the run time such as to overcome the attractant or repellent molecular diffusion and sense a variation in concentration. This qualitative argument provides a lower bound for the run length ($l_{run} > \sqrt{D_m t_{run}}$) where D_m is the molecular diffusion constant of the attractant (or repellent). The minimal value: $l_{run} > D_m/V_0$, typically $100\,\mu$m for an *E.coli*, is indeed the right magnitude observed.

2.5 Swimmers in interactions

Swimming micro-organisms (pusher or puller) induce a long-range flow field scaling as $\propto \sigma_0/r^2$ which interact with the other swimmers. This is a consequence of the force dipole picture. However at short distances (i.e. few bacteria body size) the effective interaction maybe different [37] and sensitive to much details involving the shape details and the swimming dynamics. The sign of the interaction (attractive or repulsive) depends on the relative angular position and on the orientation between the swimmer. An extensive discussion and references can be found in the review by Lauga et al. [21]. Following the dipolar force picture which remain essentially qualitative at short distances, two side by side pusher swimmers are attracted whereas pullers are repelled. This can be qualitatively assessed from an inspection of the flow field as displayed for pusher swimmers in Fig. 1(c) (for pullers, the flow lines are reversed). For micro-organisms swimming in line along the same direction, it is the opposite: pullers have the tendency to stay in lines while for pushers, this configuration is unstable as they repel each others. Also, since hydrodynamic shear, induces a solid rotation of elongated objects, two pushers moving with some relative angle along the same direction, will feel a torque that has the tendency to align them. Therefore they will finally swim, for a while, in parallel. This is indeed an important element participating to the onset of collective motion as observed for concentrated suspensions of such micro-organisms (see infra).

Similarly, for bacteria swimming close to a solid surface, the pusher/puller distinction has a determinant influence. A bacterium moving close to a solid surface, for which the fluid boundary condition is a zero velocity, will "see" its hydrodynamic image. Consequently, pusher swimmers have the tendency to align along the surface and be attracted by hydrodynamic forces [47–49]. For puller swimmer, the perpendicular position is more favourable. Moreover, the elongated shape of most bacteria will further contribute to a nematic alignment with the surface simply by steric interactions (due to the impenetrability of the solid surface). Therefore, due to these effects, of both hydrodynamics and kinetic origins, pusher bacteria spend a long time

swimming in the surface vicinity and thus their concentration displays a significant increase nearby solid surfaces [47–49].

In the context of suspensions of active swimmers, is important to notice that the density of micro-organisms is often characterized by a volume fraction based on a body volume $\mathcal{V}_b$:

$$\phi = n\mathcal{V}_b \tag{9}$$

where n is the number density and in the following, we use this definition to characterize the suspension concentration. For $E.coli$ $\mathcal{V}_b = 1\,\mu\mathrm{m}^3$. However, to assess a situation that is really dilute, i.e. where steric or hydrodynamic interactions between bacteria can be seen as marginal, it is important to keep in mind that it is better to consider an excluded volume based on a sphere with a diameter l corresponding to the total swimmer size, including the flagella:

$$\nu = n\frac{\pi}{6}l^3 \approx \phi\left(\frac{l}{a}\right)^3 \tag{10}$$

with $a \approx \mathcal{V}_b^{1/3}$ the typical body size. The transition from dilute to semi-dilute regime is then occurring for the condition $\nu = O(1)$, which corresponds in practice, to very small values of ϕ.

2.6 Collective organization

For bacteria suspensions, a natural aptitudes to undergo collective motion was identified by many experiments [13–16] and also by numerical simulations [38–40]. From a conceptual point of view, the issue of collective organization for pushers can be simply viewed as a result of the hydrodynamic interactions between the swimmers. This picture ignores other possible sources of interaction via for example, the release of attractive chemicals by the bacteria. However, as a purely mechanical phenomenon, it can be addressed theoretically by a stability analysis of the hydrodynamic modes and complemented by numerical simulations to understand the dynamics beyond the linear regime [38–42]. An important outcome of these studies is that for rear-activated swimmers, a long range nematic ordering as well as a fully randomly oriented state are both unstable and essentially will lead to mesoscopic collective motion [40,41]. When concentration is increased, the existence of a well define volume fraction, at which collective motion should apprear (as predicted for example by Subramanian and Koch [42]) is still debated. In a recent contribution Saintillan and Shelley [40] studied numerically the emergence of a correlated dynamics solely caused by hydrodynamic interactions (slender-body swimmers). For pushers, they show a progressive increase with concentration of the velocity correlation lengths when going from the dilute to the semi-dilute regime. This progressive appearance of collective motion without a clear threshold, was recovered experimentally with $E.coli$ in 3D [16]. Qualitatively, the experimental observations witness a qualitative difference between the more dilute case showing small clusters of co-moving bacteria and the higher concentration where large scale collective motion appears (see Fig. 2). Note that in more confined environments (quasi 2D films or confined cells), the occurrence of a density threshold for collective motion was reported [43,44]. Reasons for a difference with the 3D situation are still unclear.
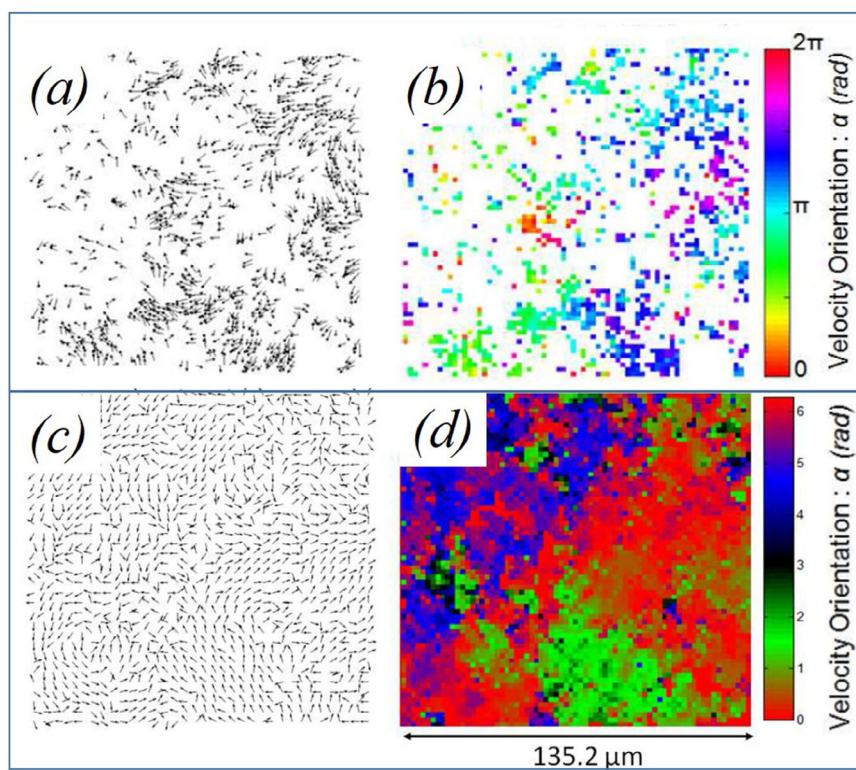
Fig. 2. Collective organization of *E.coli* bacteria (top panels volume fraction $\phi = 8.0 \ 10^{-3}$ and bottom panels $\phi = 2.0 \ 10^{-2}$ in absence of flow. The left pictures correspond to the bacteria velocity fields obtained by PIV measurements. The right pictures are the corresponding orientations α with respect to the horizontal direction and displayed in a colour map. Patches of similar colour of size much larger than a bacterium body size, witness of the large scale collective motion (see Gachelin et al. [16]).

3 Statistical mechanics of active suspensions: the emergence of an "active fluid"

3.1 A simple kinetic model for dilute active suspensions

There are different view points suited to handle the hydrodynamics of active fluids. First the macroscopic phenomenology approach as exposed for example in the review by Marchetti et al. [3]. In a nut-shell, this type of approach identifies the relevant terms in the density and momentum transport equations. Stemming from general symmetry argument rendering the generic nature of the interactions, these fields are coupled with the relevant order parameters such as the polar direction of motion or the nematic alignment tensor. To close the theory, dynamical equations for the order parameters are added to the description. The second approach is more "bottom-up" or "micro/macro" in the statistical mechanics jargon, as it describes more precisely the microscopic behaviour and interactions between the swimmers, averaged to obtain the macroscopic contributions to transport (see review by Marenduzzo et al. [71] in this series for a more complete picture). At the end, both approaches should provide similar macroscopic outcome; however the micro/macro path is clearly more difficult to handle when multiple interactions become significant. On the other hand,

it provides testable predictions for the constitutive relations involving well identified microscopic scale parameters.

Here we will only give an outlook for the simplest kinetic model aiming at establishing from the microscopic swimming properties, the viscosity of a dilute bacterial suspension in a flow. We will follow essentially the approach developed by Haines et al. [55] or Saintillan [56] and provide qualitative and heuristic arguments to justify the generic form of the viscous response. For more technical details, we recommend the reading these two articles or for example, a summarized version in a review by Saintillan and Shelley [45].

In the dilute limit, interactions between bacteria can be neglected and the transport is modelled first by assuming that the local bacteria velocity is the vectorial sum of the swimming velocity $\boldsymbol{v}_0$ and the flow velocity $\boldsymbol{v}_F$:

$$\boldsymbol{v}(\boldsymbol{r}) = \boldsymbol{v}_0 + \boldsymbol{v}_F. \tag{11}$$

In a flow, the local shear rate induces a rotation of the body. The motion of the bacteria director $\boldsymbol{p}$ (the unit vector along the tail/head direction) can be represented at the most simple level, by a Fokker-Planck equation on the probability density for the director orientation $P(\boldsymbol{p})$:

$$\dot{P} + \boldsymbol{\nabla}(\dot{\boldsymbol{p}}P) - D_r \nabla^2 P = 0 \tag{12}$$

where D_r is an angular diffusion constant.

Note here, the alternative and somehow more refined picture initially proposed by Subramanian and Koch [42] accounting explicitly for the run & tumble process in Eq. (12). They argue that this process is essentially different from the continuous reorientation due to Brownian motion and introduce in Eq. (12) two additional terms, one for the orientation loss at the tumbling rate and a second one, for the orientation gain stemming from a kernel describing jumps in orientation. A generic form for this kernel is proposed to encompass situations ranging from random motion to persistent swimming. However in the simple and heuristic presentation of this review, we will only consider in (12) an effective rotation diffusion term accounting for all disorientation contributions either due to Brownian effects or to active tumbling processes.

The orientation kinematics (in absence of noise) of an elongated axisymmetric particle in a shear flow is usually modelled by the Bretherton-Jeffery equation [52,53]:

$$\dot{\boldsymbol{p}} = (\bar{\bar{1}} - \boldsymbol{p}\boldsymbol{p})(\beta \bar{\bar{E}} + \bar{\bar{W}})\boldsymbol{p}. \tag{13}$$

$\beta = \frac{r^2-1}{r^2+1}$ is the Bretherton constant characterizing the shape via the aspect ratio $r = l/a$; $\bar{\bar{E}}$ and $\bar{\bar{W}}$ are respectively the shear and the rotation rate tensors. In a simple shear geometry, characterized by the shear rate $\dot{\gamma}$, the most important outcome of such a model is an interplay between shear rate aligning the elongated bacteria along the flow direction at a time scale $\dot{\gamma}^{-1}$ and active tumbling processes disorienting the bacteria at a time scale D_r^{-1}. The mean orientation of the bacteria under shear is controlled by a rotational Péclet number:

$$P_e = \frac{\dot{\gamma}}{D_r}. \tag{14}$$

The mean desorientation angle (i.e. not along the flow) $\bar{\theta}$ is actually maximal when $P_e = O(1)$. At large P_e a bacterium is oriented preferentially along the flow and the mean angle goes to zero with a scaling:
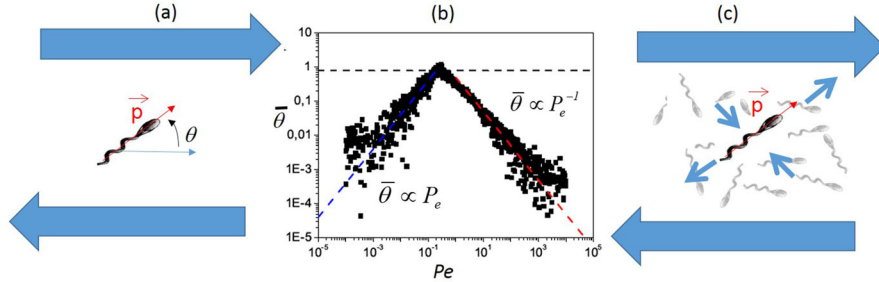
$$\bar{\theta} \propto P_e^{-1}, \ P_e \gg 1. \tag{15}$$

Fig. 3. Swimming and tumbling in a simple shear flow. (a) Schematic representation of a bacterium swimming at an angle θ with respect to the shear direction. (b) Result of numerical simulations of the Bretherton-Jeffery equation [51] in a simple shear and for a Poisson distribution of run times (average t_{run}) and random reorientation. The mean orientation angle $\bar{\theta}$ is displayed as a function of the Péclet number $P_e = \dot{\gamma} t_{run}$. The two regimes low shear ($\propto P_e$) and high shear ($\propto P_e^{-1}$) are displayed. The dotted horizontal line is $\bar{\theta} = \pi/4$. (c) Schematics of the flow directions induced by a "pusher" swimmer oriented at an angle θ. Qualitatively, when the swimmer is oriented with an angle $\pi/4$, the motive action of the flow "helps" to shear, therefore the effective viscosity decreases.

similarly, at low P_e, the disorientation process due to the tumbling dominates and the mean orientation angle vanishes with a linear scaling:

$$\bar{\theta} \propto P_e, \ P_e \ll 1. \tag{16}$$

An illustration of this scaling behaviour is displayed in Fig. 3(c). The mean orientation angle is extracted from solving numerically a Bretherton-Jeffery equation with a Poissonian distribution of run times followed by a random reorientation of the swimming direction [51]. The Bretherton constant used in this example is $\beta = 0.6$.

In addition, as underlined by Zoetl et al. [46], in confined flows displaying a shear-gradient such a Poiseuille flows, families of quasi-periodic trajectories appear as a result of the shear gradient experienced by the swimmers. This result indicates that the transport and dispersion properties of active suspensions are in this case non trivial. This is currently a very open problem which outcome turns out to be qualitatively different from the standard hydrodynamic transport of passive colloidal particles [50].

In the following, we will review and discuss two situations. The first is an homogeneous shear which is the case of rheometric devices such as cone-plane geometries or Couette shear cells. The second case is a microfluidic Hele-Shaw channel displaying a Poiseuille parabolic flow, a generic situation which opens the discussion on the more general issue of transport in confined environments such as capillary tubes or porous media.

3.2 Viscosity of active suspensions in the dilute regime: the outcome of the kinetic models

Following the scheme of calculation developed by Hinch and Leal [61] to understand the rheology of fibers, the shear stress contribution $\bar{\bar{\Sigma}}$ of the swimming dipole will add-up to the viscous contribution of the solvent. In the dilute regime, if Brownian motion is neglected, the stress tensor can be decomposed into two additive part:

$$\bar{\bar{\Sigma}} = \bar{\bar{\Sigma}}_p + \bar{\bar{\Sigma}}_a \tag{17}$$

where $\bar{\bar{\Sigma}}_p$ is a passive contribution coming from the particle drag and $\bar{\bar{\Sigma}}_a$ is the active part which can be written, for a density n of bacteria bearing a dipolar strength σ_0:

$$\bar{\bar{\Sigma}}_a \propto \epsilon n \sigma_0 \int d\boldsymbol{p}(\bar{\bar{I}}/3 - \boldsymbol{p}\boldsymbol{p})P(\boldsymbol{p}) \tag{18}$$

where the average is taken over all the swimming orientations $P(\boldsymbol{p})$. The interpretation of the active shear stress contribution Σ_a is straightforward as $n\sigma_0$ can be seen as a volumic density of energy to move the fluid at the scale of a bacterium. Note that the prefactor's sign ϵ in Eq. (18) is positive for pullers and negative for pushers. The magnitude of the passive part Σ_p, is $n\eta_0 l^3 \dot{\gamma}$ and corresponds to the viscous energy loss per unit volume.

Now the question is to understand the relative contribution of both terms, active and passive on the effective viscosity to be added to the solvent viscosity η_0. For the passive part, the contribution is $\Sigma_p/\dot{\gamma} \propto \eta_0 l^3 \propto \eta_0 \phi$. For the active part Σ_a, the contribution to viscosity is: $n\sigma_0/\dot{\gamma}$ and will depend on the effective mean orientation of the bacteria in the flow. Now, *at low shear rate*, one can make the following heuristic argument. As displayed on Fig. 3, the bacteria still orient in average off the flow direction, with a mean angle proportional to the shear rate (Eq. (16)). The active contribution to the suspension viscosity being $\eta_a = \frac{\Sigma_a}{\dot{\gamma}}$, it is easy to get from symmetry arguments that the tensorial part of Eq. (18) will yield a term proportional to P_e and thus, when $P_e \to 0$, $\eta_a \to \epsilon \, n\sigma_0/D_r$. The active contribution converges to a constant value Note that the sign ϵ of this contribution to viscosity differs for "pusher" and "puller" swimmers.

More quantitatively, using the previously exposed simple representation for the swimming kinematics, several theories [55–57] were developed for the dilute regime. The suspension viscosity η was predicted as a function of the two dimensionless Péclet numbers of the problem: $P_e = \dot{\gamma}/D_r$ defined earlier and the second one:

$$P_e^b = \frac{V_0}{l \, D_r} \tag{19}$$

which involves the hydrodynamic time: $t_c = \frac{l}{V_0}$ for a bacterium to move over its own size. The relative viscosity can be cast the general form:

$$\frac{\eta}{\eta_0} = 1 - \Psi(P_e, P_e^b)\phi \tag{20}$$

where $\Psi(P_e, P_e^b)$ a dimensionless function. Also in their own framework, Subramanian and Koch [42] derived and expression for the linear viscous response of the hydrodynamic modes. Their description eventually includes more details on the run/tumble dynamics but turns out to be essentially similar.

The outcome of the theories are (i) at high shear rate ($\dot{\gamma}t_c = P_e/P_e^b > 1$) the active contribution to viscosity is negligible and the viscosity becomes akin to suspensions of passive particles of the same shape as the bacteria; (ii) below a shear rate value $\dot{\gamma}_c t_c = O(1)$ the suspension viscosity becomes lower than the suspending fluid viscosity; (iii) at low shear rate ($P_e \ll 1$), an active Newtonian plateau of viscosity η_p is reached (as explained qualitatively earlier) and then can be written:

$$\frac{\eta_p}{\eta_0} = 1 + (A + \epsilon B P_e^b)\phi \tag{21}$$

where A and B are positive constants of order one and solely determined by the micro-organism shape. Note that for pusher swimmers ($\epsilon = -1$), the prefactor in front

of ϕ may become negative for large values of P_e^b, yielding a volume fraction above which, the plateau viscosity η_p becomes lower than the suspending fluid viscosity η_0. Note that Hatwalne et al. [58] also predicted using mean-field phenomenological hydrodynamic equations, the possible decrease of viscosity with concentration for active pusher suspensions and the opposite behaviour for pullers.

4 Viscosity of active bacterial suspensions: experiments

Experimental evidence for viscosity reduction was first found for *Bacillus subtilis* [17] and then for *E. coli* [18]. It is only recently that a full rheological characterization (viscosity *versus* shear rate) was provided as a direct test for the kinetic theory for the viscous response under simple shear [19].

4.1 Maintaining the activity of a bacterial suspensions

As for any biological material, the question of maintaining a constant activity in a controlled environment is a crucial issue to the completion of significant experimental work. To perform laboratory experiments with bacteria suspensions, it is important to keep in mind that in a food rich medium, a population will double in typically 20 min (at 30 °C). Thus to avoid such a Malthusian growth, one needs to suspend the bacteria in a "minimal medium" suited to provide enough elements to maintain a swimming activity but discourage the cell growth. However, when deprived of O_2 many bacteria strains such as *E.coli* can change their motility characteristics in a few minutes and eventually stop swimming [60]. However, it is worth noticing that in soft micro-fluidic devices made of PDMS, gases like O_2 can go through the polymeric structure. So in a large range of concentration, bacteria can access O_2 in sufficient amount. Note also that some species such as *Bacillus subtilis* are extremely sensitive to O_2 shortage and for this reason, are delicate to handle in microfluidic devices even in PDMS. In the following, we will discuss essentially of *E.coli* strains.

To characterize the activity in various environments, by tracking hundreds of trajectories, the mean square displacement was computed as a function of time and the corresponding velocities V_0 as well as the translational diffusion coefficients D_t are reported in Fig. 4. To keep a constant activity in a closed environment, L-serine can be added to the suspension. This is an amino-acid allowing the bacteria to swim in absence of oxygen [59,60]. Thus a good and constant activity level can be kept for at least half an hour in a large concentration range. Note that the V_0 and D_t values are lower than the corresponding values in presence of O_2. The results presented in the following, were obtained with two wild type *E.coli* (ATCC9637 and RP437). These strains have slightly different shapes and activities.

4.2 Low-shear rheometry

In Lopez et al. [19], to assess the full reological response of *E.coli* suspensions, rheometric measurements were performed in a low-shear Taylor-Couette shear device. To be able to reach the active plateau, one has a-priori to go to very low shear rates ($Pe < 1$ implies $\dot{\gamma} < 0.1\,\mathrm{s}^{-1}$) and measure viscosities of the order or less than the viscosity of water ($10^{-3}\,\mathrm{Pa.s}$). This is difficult with conventional rheometers. The configuration of a low-shear viscometer allowing such measurements, is an external cylinder that rotates at an angular rotation rate Ω. The inner cylinder is suspended via a torsion wire and its angular position is maintained constant via a feedback loop
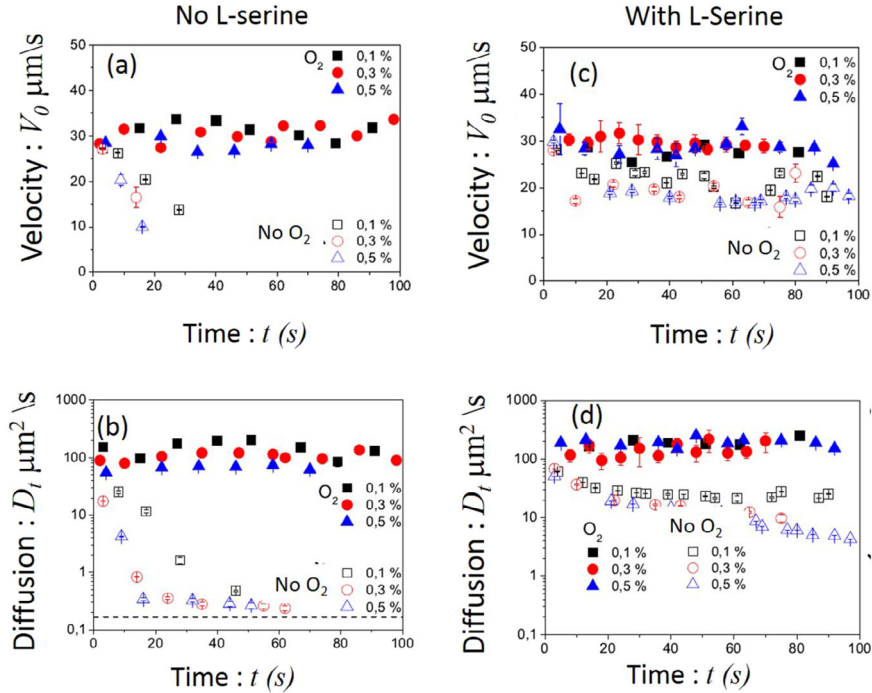
Fig. 4. Activity characterization of *E.coli* (ATCC9637) suspensions under different environmental conditions. From the mean square displacement of hundreds of tracks, the swimming velocities and the translation diffusivity coefficients are extracted (see Eq. (8)), without (a),(b) and with (c),(d) L-serine. L-serine is an amino-acid replacing in anaerobic conditions, O_2 in the respiration path. In absence of L-serine and O_2, the bacteria asphyxiate and the activity drops down in a few minutes. However with L-serine, even in absence of O_2, a significant activity is maintained [51].

by exerting a compensating torque. Due to the feedback, the torque exerted on the inner cylinder is obtained with very high precision. The gap ($h = 500 \, \mu$m) is significantly smaller than the cylinder radius ($R = 5.5$ mm) and therefore at constant Ω, the shear rate is homogeneous and very well defined. Given a shear stress σ measured for an imposed shear rate $\dot{\gamma}$ an effective viscosity $\eta = \sigma/\dot{\gamma}$ is then obtained.

4.3 Viscous response

For the suspending fluid alone (a Newtonian fluid, $\eta_0 = 1.4$ mPa.s), stress time-responses at the start or at the stop of the applied shear are fast and correspond to the device compliance (grey and black lines in Fig. 5(b)). A similar behaviour is observed for the bacterial suspensions probed at high shear rates which moreover display a viscosity higher than η_0 as generically observed for passive particle suspensions. But for low shear rates, a strikingly different behaviour shows up. When shear starts, the stress jumps and then, after an exponential decrease lasting a few seconds, it reaches a steady effective viscosity. When shear stops, the stress decreases abruptly to eventually change sign. In this last case, the bacteria motion induces a motive stress on the Taylor-Couette device. Thereafter, the trajectory randomization processes affect the swimming direction and stress relaxes exponentially to 0. In the framework of a rotational diffusion equation describing the bacteria desorientation with a diffusion
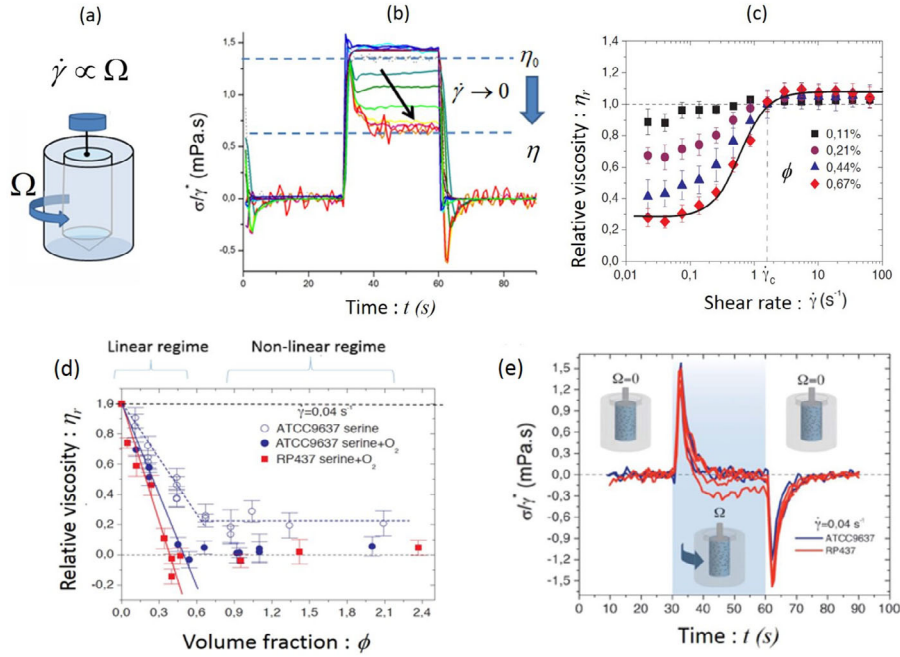
Fig. 5. Low shear rheometry [19]. (a) Schematics of the Couette-shear apparatus. (b) Response of an *E.coli* suspension ($\phi = 2.0 \ 10^{-3}$ to different shear rates $\dot{\gamma}$. (c) Rheogram for the relative viscosity: η/η_0 vs $\dot{\gamma}$ at different concentrations ϕ. (d) Linear and non-linear viscous response for two strains of *E.coli* (ATCC9637 and RP437) [19]. The active plateau relative viscosity η_p/η_0 is displayed as a function of the concentration ϕ. (e) Viscous response at $\dot{\gamma} = 4.0 \ 10^{-2} s^{-1}$ for ATCC9637 and RP437 in the non-linear regime.

constant D_r, the characteristic time τ_r would be: $\tau_r = \frac{1}{2D_r}$ [28]. Here $\tau_r \simeq 2.4 \pm 0.3$ s corresponding to a rotational diffusion value ($D_r \approx 0.5 \, \text{rd}^2/\text{s}$) smaller than what has been currently reported for wild-type *E.coli* undergoing run-tumble motion [28].

Figure 5(c) displays a full rheogram i.e. the suspension viscosity η as a function of $\dot{\gamma}$ for different volume fractions ranging from $\phi = 0.11\%$ (1.1×10^9 bact/mL) up to $\phi = 0.67 \%$ (6.7×10^9 bact/mL). At low shear rate the "active viscous plateau" $\eta_p(\phi)$ appears. As predicted, $\eta_p(\phi)$ decreases linearly with the concentration (see Fig. 5(a) in the linear regime).

4.4 The non-linear and semi-dilute regime

When the bacteria volume fraction is further increased, viscosity becomes independent of the concentration (Fig. 5(d)). This is suggesting a transition between a dilute and a semi-dilute regime. Indeed, this last regime is not predicted by dilute suspension theories for which the viscous response should remain linear in concentration. Non-linear effects may come into play as the flow induced by the swimming bacteria may strongly influence the mean shear flow responsible for the bacteria orientation. It is also a regime where clustering interactions leading to collective motion would come into play [16]. For the ATCC9637 strain in a medium that doesn't contain oxygen, this regime appears at $\phi > 0.7\%$ and $\eta_p/\eta_0 \sim 0.2$. In oxygenated conditions and for highly motile strains, the viscosity η_p/η_0 reaches a constant value ~ 0 for $\phi \sim 0.5\%$ and $\phi \sim 0.4\%$ for ATCC9637 and RP437 respectively. It means that over a significant
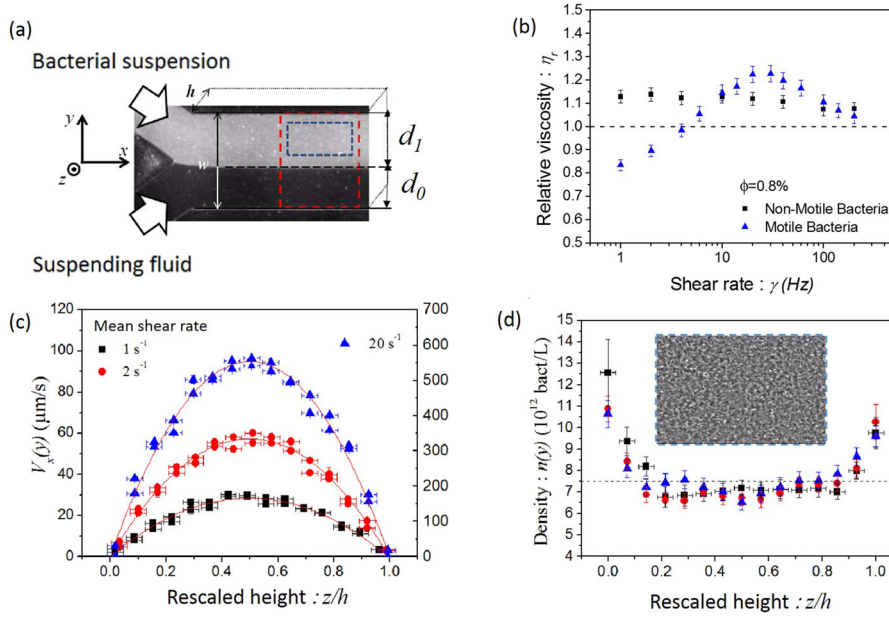
Fig. 6. Micro-fluidic rheometry of a wild-type ATCC9637 *E.coli* suspension(see [18]). (a) Sketch of the set-up and methodology to extract the interface position. (b) Relative viscosity as a function of shear rate for motile and non motile *E.coli.* (c) Flow profile $V_x(z)$, obtained by tracking passive $2\,\mu$m latex spheres at different flow rates Q. Bacteria concentration profile $n(z)$ at different flow rates Q.

range of concentration, one obtains a viscous response such that the local viscous dissipation is macroscopically entirely compensated by the swimming activity.

4.5 Microfluidic rheometry

The previous measurements where made in a device producing a simple shear. In a confined environment as a micro-fluidic Hele-Shaw channel, the basic flow profile is parabolic and the question is whether an active viscous response as described before, can also manifest itself at low shear rate. To probe the emergence of such an "active viscosity", a micro-fluidic system initially proposed by Guillot and collaborators [62–64], was built. These authors have shown that a Y shape micro-fluidic channel is well suited to compare the viscosities of two simple liquids at low shear. An adaptation of such a device to bacterial fluids was done by Gachelin et al. [18] (see Fig. 6). On one arm, the active suspension is injected and on the other arm, the suspending fluid in injected at the same flow rate Q. The channel thickness is $h = 100\,\mu$m and the width $W = 600\,\mu$m. From the position of the interface between the pure fluid and the suspension, one may extract the suspension relative viscosity. The channel widths being respectively d_0 (pure fluid) and d_1 (suspensions), one has $Q = \frac{h^3 d_0}{12\eta_0}\partial P/\partial x$. The pressure gradients are identical on both sides of the interface, the relative viscosity is thus obtained as:

$$\frac{\eta}{\eta_0} = \frac{d_1}{d_0}. \tag{22}$$

This measured value of relative viscosity can be associated with a shear rate: $\dot{\gamma}_M = 6Q/h^2 d_1$. As displayed in Fig. 6, the effective viscosity rheogram shows a

non-Newtonian viscosity. Varying the bacteria density and the flow rate, one can observe a regime specific to active fluids, where the relative viscosity is lower than the viscosity of the suspending viscous fluid.

Such micro-fluidic devices also have the advantage of allowing a direct visualization of the bacteria in the fluid. Using a fast camera coupled to the microscope, the vertical profiles for the bacteria density and the corresponding velocity distributions for both the fluid (tracking passive tracers) and the bacteria, can be obtained. The measurements show as expected that the basic flow profile is not significantly affected by the weak non-Newtonian character of the active suspensions. However, the technical limitations due to the dynamical stability of syringes undergoing stick-slip motion at low flow rates, has prevented so far to explore the very low shear-rate regime.

5 Conclusion

In conclusion, the aim of this paper was to establish an elementary connection between a simple vision of the statistical mechanics of active fluids under flow and recent experiments with bacteria suspensions. Interestingly, in the dilute limit, a good agreement between model predictions and experimental measurements was reached. The viscosity rheograms turn out to be similar. At low-shear, the viscosity is found to decrease with concentration at values lower than the suspending fluid viscosity. It is also interesting that such a peculiar behaviour can be found also in microfluidic geometries where the shear-rate is not uniform. The most striking feature of the experimental rheological response is the emergence of a viscousless "superfluidity" regime, in a large range of concentrations. Presently, there is no hydrodynamic calculation describing the impact of bacteria interactions and the possible influence of collective organization on the macroscopic rheology to predict such a regime. However, there are some arguments based on the emergence of coupling terms in phenomenological transport equations, pointing on the possibility of a transition to a zero-viscosity regime [65–67]. It would be interesting to confront directly these predictions, and most of all, identify precisely the spontaneous collective organization processes undertaken by the bacteria in the flow when reaching the viscousless regime. In the framework of the low shear rheometric device used by Lopez et al. [19], it is so far impossible to visualise in-situ the organization of the bacteria. However, the fact that an active viscosity regime was already identified for a micro-fluidic channel is encouraging. Recently there was a theoretical calculation confirming the decrease of effective viscosity with concentration in Hele-Shaw cells and the existence of a low shear viscous plateau [72]. The experimental challenge would be now to push the measurements towards the onset for a zero-viscosity transition if it exists in this geometry.

References

1. T. Vicsek, A. Zafeiris, Phys. Rep. **517**, 71 (2012)
2. P.W. Anderson, Science **177**, 393 (1972)
3. C. Marchetti et al., Rev. Mod. Phys. **85**, 1143 (2013)

4. A. Baskaran, M.C. Marchetti, Proc. Natl. Acad. Sci. USA **106**, 15567 (2009)
5. X.-L. Wu, A. Libchaber, Phys. Rev. Lett. **84**, 3017 (2000)
6. G. Mino et al., Phys. Rev. Lett. **106**, 048102 (2011)
7. L.G. Wilson et al., Phys. Rev. Lett. **106**, 018101 (2011)
8. P. Galajda, J. Kleymer, P. Chaikin, R. Austin, J. Bacteriol. **189**, 8704 (2007)
9. E. Hulme et al., Lab Chip **8**, 1888 (2008).
10. J. Hill, O. Kalkanci, J.L. McMurry, H. Koser, Phys. Rev. Lett. **98**, 068101 (2007)
11. E. Altshuler et al., Soft-Matter **9**, 1864 (2013)
12. R. Rusconi, J.S. Guasto, R. Stocker, Nat. Phys. **10**, 494 (2014)
13. C. Dombrowski et al., Phys. Rev. Lett. **93**, 098103(2004)
14. A. Sokolov, I.S. Aranson, Phys. Rev. Lett. **109**, 248109 (2012)
15. J. Dunkel et al., Phys. Rev. Lett. **110**, 228102 (2013)
16. J. Gachelin, A. Rousselet, A. Lindner, E. Clement, New J. Phys. **16**, 025003 (2014)
17. A. Sokolov et al., Phys. Rev. Lett. **103**, 148101 (2009)
18. J. Gachelin et al., Phys. Rev. Lett. **110**, 268103 (2013)
19. H.M. Lopez, J. Gachelin, C. Douarche, H. Auradou, E. Clement, Phys. Rev. Lett. **115**, 028301 (2015).
20. E.M. Purcell, Am. J. Phys. **45**, 11 (1997)
21. E. Lauga, T. Powers, Rep. Prog. Phys. **72**, 096601 (2009)
22. S. Childress, *Mechanics of Swimming and Flying* (Cambridge University Press, Cambridge, 1981)
23. H.C. Berg, *E.coli in Motion* (Springer-Verlag, New York, 2004)
24. V. Martinez et al., Proc. Natl. Acad. Sci. USA **111**, 17771 (2014)
25. J.S. Guasto, K.A. Johnson, J.P. Gollub, Phys. Rev. Lett. **105**, 168102 (2010)
26. K. Drescher et al., Phys. Rev. Lett. **105**, 168101 (2010)
27. K. Drescher et al., Proc. Natl. Acad. Sci. USA **108**, 10940 (2011)
28. J. Saragosti, P. Silberzan, A. Buguin, PLoS ONE **7**, e35412 (2012)
29. V.A. Martinez et al., Biophys. J. **103**, 16371647 (2012)
30. H.C. Berg, D.A. Brown, Nature **239**, 500 (1972)
31. K. Son, J.S. Guasto, R. Stocker, Nat. Phys. **9**, 494 (2013)
32. R.E. Goldstein, M. Polin, I. Tuval, Phys. Rev. Lett. **103**, 168103 (2009)
33. S.H. Larsen, R.W. Reader, E.N. Kort, W.W. Tso, J. Adler, Nature **249**, 7477 (1974)
34. M. Schnitzer, Phys. Rev. E **48**, 25532568 (1993)
35. M.J. Tindall, P.K. Maini, S.L. Porter, J.P. Armitage, Bull. Math. Biol. **70**, 1570 (2008)
36. G.H. Wadhams, J.P. Armitage, Nat. Rev. Mol. Cell Biol. **5**, 1024 (2004)
37. L. Qian et al., Phys. Fluids **19**, 061701 (2007)
38. J.P. Hernández-Ortiz, C.G. Stoltz, M.D. Graham, Phys. Rev. Lett. **95**, 204501 (2005)
39. D. Saintillan, M.J. Shelley, Phys. Rev. Lett. **99**, 058102 (2007)
40. D. Saintillan, M.J. Shelley, J. R. Soc. Interface **9**, 571 (2012)
41. R.A. Simha, S. Ramaswamy, Phys. Rev. Lett. **89**, 058101 (2002)
42. G. Subramanian, D.L. Koch, J. Fluid Mech. **632**, 359 (2009)
43. A. Sokolov, I.S. Aranson, J.O. Kessler, R.E. Goldstein. Phys. Rev. Lett. **98**, 158102 (2007)
44. H.P. Zhang, A. Be'er, E.-L. Florin, H.L. Swinney, PNAS **107**, 13626 (2010)
45. D. Saintillan, M.J. Shelley, C.R. Phys. **14**, 497 (2013)
46. A. Zöttl, H. Stark, Phys. Rev. Lett. **108**, 218104 (2012)
47. A.P. Berke, L. Turner, H.C. Berg, E. Lauga, Phys. Rev. Lett. **101**, 038102 (2008)
48. G. Li, J.X. Tang, Phys. Rev. Lett. **103**, 078101 (2009)
49. J. Elgeti, G. Gompper, Europhys Lett. **85**, 38002 (2009)
50. B. Ezhilan, D. Saintillan, J. Fluid Mech. **777**, 482 (2015)
51. J. Gachelin, PhD. thesis, University Pierre et Marie Curie (2014)
52. G.B. Jeffery, Proc. R. Soc. A **102**, 161 (1922)
53. F.P. Bretherton, J. Fluid Mech. **14**, 284 (1962)
54. S. Rafaï, L. Jibuti, P. Peyla, Phys. Rev. Lett. **104**, 098102 (2010)
55. B.M. Haines et al., Phys. Rev. E **80**, 041922 (2009)

56. D. Saintillan, Exp. Mech. **50**, 125 (2010)
57. S.D. Ryan et al., Phys. Rev. E **83**, 050904(R) (2011)
58. Y. Hatwalne, S. Ramaswamy, M. Rao, R.A. Simha, Phys. Rev. Lett. **92**, 118101 (2004)
59. J. Adler, J. Bacteriol. **92,** 121 (1966)
60. C. Douarche, A. Buguin, H. Salman, A. Libchaber, Phys. Rev. Lett. **102**, 198101 (2009).
61. J. Hinch, G. Leal, J. Fluid Mech. **52**, 683 (1972)
62. P. Guillot et al., Langmuir **22**, 6438 (2006)
63. P. Galambos, F. Forster, *Micro-Electro-Mechanicical System (MEMS)* (1998), p. 187 (unpublished)
64. P. Nghe, P. Tabeling, A. Ajdari, J. Non-Newtonian Fluid Mech. **165**, 313 (2010)
65. M.E. Cates, S.M. Fielding, D. Marenduzzo, E. Orlandini, J.M. Yeomans, Phys. Rev. Lett. **101**, 068102 (2008)
66. L. Giomi, T.B. Liverpool, M.C. Marchetti, Phys. Rev. E **81**, 051908 (2010)
67. S. Fürthauer, M. Neef, S.W. Grill, K. Kruse, F. Jülicher, New J. Phys. **14**, 023001 (2012)
68. R.G. Winkler, Eur. Phys. J. Special Topics **225**, 2079 (2016)
69. U.B. Kaupp, L. Alvarez, Eur. Phys. J. Special Topics **225**, 2119 (2016)
70. R. Jeanneret, M. Contino, M. Polin, Eur. Phys. J. Special Topics **225**, 2141 (2016)
71. D. Marenduzzo et al., Eur. Phys. J. Special Topics (2016)
72. R. Alonso-Matilla, B. Ezhilan, D. Saintillan, Biomicrofluidics **10**, 043505 (2016)